



Observation of the GZK Cutoff by the HiRes Experiment

D. R. BERGMAN¹, FOR THE HIGH RESOLUTION FLY'S EYE COLLABORATION

¹*Rutgers — The State University of New Jersey, Dept. of Physics and Astronomy, Piscataway, NJ, USA*
bergman@physics.rutgers.edu

Abstract: HiRes has observed the GZK cutoff. HiRes observes two separate features in the ultra-high energy cosmic ray (UHECR) energy spectrum: a hardening of the spectrum, the ankle, at an energy of 4×10^{18} eV, and a sharp reduction in the flux at higher energies, above 6×10^{19} eV. This reduction in the flux, given the primarily light measured composition, is at just the right energy to be caused by the GZK energy loss mechanism. We present the latest HiRes monocular spectra, a description of our systematic uncertainties, the aperture calculation and its verification, and fits to the spectrum to estimate the statistical significance of the observed features and their positions.

The GZK cutoff was predicted over 40 years ago, when Greisen [1], along with Zatsepin and Kuzmin [2], observed that the extragalactic flux of protons with energies above 6×10^{19} eV would be sharply reduced by energy losses from photo-pion production of protons on the cosmic microwave background. The High Resolution Fly's Eye Experiment (HiRes) has now collected sufficient data to observe the predicted cutoff.

In this presentation, we examine the procedure for determining energies with the HiRes detectors in monocular observation. Equally important is the calculation of the aperture, which varies with energy. It is the absence of events that we take as evidence of a cutoff, so we must accurately know the aperture to draw this conclusion.

The data shown here are identical to those presented in [3]. This includes monocular spectra from each of HiRes-I and HiRes-II. The HiRes-I spectrum includes data taken between May 1997 and June 2005. The HiRes-II spectrum includes data taken between December 1999 and August 2004.

Monocular reconstruction is discussed in detail in our previous publications [4, 5]; we present only a summary here. One determines the geometry of an extensive air shower in monocular mode by fitting the PMT trigger times as a function of the viewing angle. With the geometry determined, the photoelectron count is then converted to a shower size at

each atmospheric depth, using the known geometry of the shower, and corrected for atmospheric attenuation. We integrate the resulting function over the shower depth, X (using the determined values of N_{\max} and X_{\max}), and then multiply by the average energy loss per particle to give the visible shower energy. A correction for energy carried off by non-observable particles to give the total shower energy ($\sim 10\%$) [6] is then applied.

HiRes-I events are too short in angular extent for reliable determination of the geometry by timing alone. Instead, the expected form of the shower development itself is used to constrain the time fit and yield realistic geometries. The expected shower profile is taken to be the Gaisser-Hillas parameterization [7], which has been shown to be in good agreement with previous HiRes measurements [8].

Systematic Errors

The signal recorded in HiRes PMT's depends on a number of factors: the fraction of the shower energy which does not go into exciting air fluorescence, the energy loss rate of shower particles, the fluorescence yield, the transparency of the atmosphere, and the efficiency of the light collection system. Most of these factors (e.g. mean energy loss rate, fluorescence yield) give rise to an overall

uncertainty in the energy but will not change the shape of the spectrum.

The fraction of the primary particle energy that is not observable depends on the type of the primary cosmic ray. One must thus use the average cosmic ray composition (not always well known) when calculating the aperture. This fraction also depends on the model used to simulate extensive air showers. Fortunately, most of the energy is observable, so the significant differences in missing energy between proton and iron showers, and between various models, lead to an uncertainty of only a few percent. We use a missing energy correction based on QGSJet calculations, and the composition measured by the HiRes Prototype/MIA Experiment [9] and by HiRes itself (in stereo) [10]. The differences between QGSJet and Sibyll are about 1%, while the differences between proton and iron showers are about 5% [11]. We estimate a systematic uncertainty from the missing energy correction of 5%.

The energy loss rate in the shower (dE/dX) contributes in two ways. First, it determines the shape of the reconstructed shower, as the amount of light from a given position is converted into a given number of shower particles. Second, when the shower shape is fit to the Gaisser-Hillas form [7], the average dE/dX determines the energy of the shower. We use an average dE/dX of 2.19 MeV/(g/cm²) as calculated in [6]. Recent calculations give significantly higher ($\sim 10\%$) rates, which we take as the systematic uncertainty from this factor.

The fluorescence yield connects the energy deposited in the atmosphere to the number of photons produced. There have been several recent measurements [12, 13, 14]. HiRes uses the value of [12]. If one fits the measurements, one finds that the ratio of a fit to just Kakimoto *et al* to that of a fit of all three, is 1.00 ± 0.06 . Thus, the three measurements are consistent with each other at the 6% level, which we take this as the systematic uncertainty.

The systematic uncertainty due the transparency of the atmosphere is dominated by the uncertainty in size of the aerosol component. HiRes measured the vertical aerosol optical depth (VAOD) with a bistatic LIDAR system [15, 16]. However, since some of the data from HiRes-I was collected be-

fore the LIDAR system was deployed, we have chosen to use the average VAOD in correcting the signal. We have tested the validity of this approach by analyzing some of the data from HiRes-II using the measured VAOD's rather than the average value [11]. This leads to a shift in the energy of 4% independent of energy, which we take as the systematic uncertainty.

The mirror reflectivity, filter transmission and quantum efficiency, were all measured in our photometric calibration. Xenon flash lamps and YAG lasers were used in this calibration as described in [4]. This calibration is accurate to $\sim 10\%$.

Combining all these systematic uncertainties in quadrature gives an overall, energy independent, systematic uncertainty in the energy of 17%. For a spectral index of 2.8 (which is what we measure for the slope between the ankle and the GZK cut-off) this corresponds to a 30% uncertainty in the flux.

Aperture Calculation

Calculating the aperture of a fluorescence detector in a reliable manner is the most important task in our analysis. The key to success in this process is verification through data/MC comparisons: a perfectly accurate MC simulation of the detector will give distributions of observables which are identical to those obtained in the data. The extent to which the data and MC distributions agree with each other determines the systematic uncertainty of the aperture calculation.

The most relevant distributions to consider for the aperture calculation are the distance to the shower and the angular orientation of the shower. These let one know that the calculation mimics the data by putting the right number of showers in the right places and at the right angles. Other distributions (which are not orthogonal to the above ones in determining the systematic uncertainty of the aperture calculation) validate other aspects of the calculation, such as the shower brightness (light productions, transmission and collection) and time-fitting χ^2 (geometrical resolution). Each of these comparisons is shown in [17].

At lower energies, the requirement that the peak of the shower development be observed in the de-

detector leads to differing apertures for different primary particle types. However, to calculate the correct aperture does not require that we know the exact composition of the primary cosmic rays, rather that we have the right distributions of shower maximum positions, X_{max} . A comparison of this distribution was shown in [11]. The systematic uncertainty in the aperture due to this effect is also examined in [11], and it becomes quite large at the lowest energies. Because of this we include only HiRes-II data with energies above $10^{17.5}$ eV.

In the latest set of data from HiRes-II (data collected after that shown in [5]), an additional cut was applied on the distance to the shower in order to make the aperture calculation more robust. This had the effect of reducing the aperture for this data set. The result of the aperture calculation for both HiRes-I and HiRes-II is shown in figure 1.

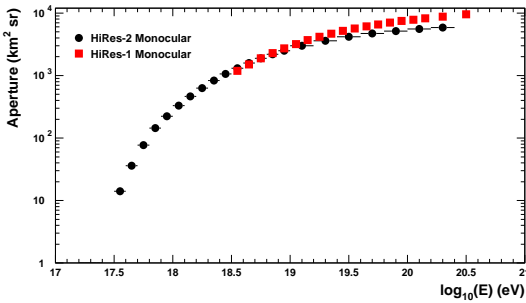


Figure 1: The apertures of the HiRes-I and HiRes-II detectors operating in monocular mode.

Monocular Spectra and Fits

The latest HiRes monocular spectra are shown in Figure 2 along with the AGASA measurement [18] for comparison.

We have fit the two HiRes monocular spectra using a binned maximum likelihood method [19], where we have included two empty bins at high energy with significant exposure for each spectrum. The fitting function was a broken power law with a changeable number of floating breakpoints. A fit with two breakpoints finds breaks at $10^{18.65 \pm 0.05}$ eV and $10^{19.75 \pm 0.04}$ eV. The spectral slopes were found to be 3.26 ± 0.02 , 2.81 ± 0.03 and 5.1 ± 0.7 , respectively. When the two spec-

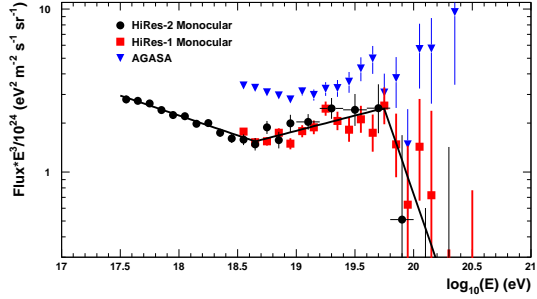


Figure 2: The cosmic-ray energy spectrum measured by the HiRes detectors operating in monocular mode. The spectrum of the HiRes-I and HiRes-II detectors are shown. The highest two energy bins for each detector are empty, with the 68% confidence level bounds shown. The spectrum of the AGASA experiment is also shown.

tra are made statistically independent by removing events-in-common from HiRes-I, the fit had a χ^2/DOF of 39.5/35. Compare this to a fit with only one breakpoint (in which the break point was found to be at the ankle) where the χ^2/DOF was 62.9/37. The χ^2 difference of 23.4, while adding two DOF, implies that the two break point fit is preferred at a confidence level corresponding to 4.5 standard deviations.

One can also calculate the number of events expected if the second breakpoint at $10^{19.75}$ eV were absent. For this calculation we extended the middle section to the highest energies without changing the spectral slope. Using the recorded exposures (with the overlap between the two detectors removed), we expect 39.9 events above $10^{19.8}$ (the lower edge of the first bin completely above the break point) from this extrapolation, where in fact we observe only 13 events. The Poisson probability for the observed deficit is $\sim 7.1 \times 10^{-7}$, which corresponds to a significance of 4.8 standard deviations, consistent with the χ^2 calculation above. Since the break occurs at the expected threshold for GZK energy loss, we conclude that the break is the GZK cutoff.

A test of this interpretation of the break as the GZK cutoff is provided by the $E_{1/2}$ criterion suggested by Berezhinsky and Grigorjeva [20]. $E_{1/2}$ refers to the energy at which the integral spectrum falls to half of what would be expected in the absence of

the GZK cutoff. Figure 3 shows the integral HiRes spectra divided by the integral of the power law spectrum used above to estimate the number of expected events above the break. From this plot, we find $E_{1/2} = 10^{19.73 \pm 0.07}$. Berezhinsky and Grigorieva predict a robust theoretical value for $E_{1/2}$ of $10^{19.72}$ eV for a wide range of spectral slopes [20]. These two values are clearly in excellent agreement, supporting our interpretation of the higher break as the GZK cutoff.

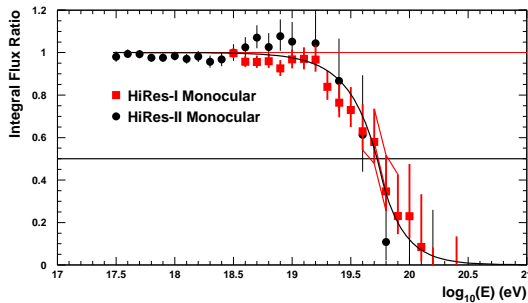


Figure 3: The HiRes monocular integral spectra, divided by the expectation from the fit in Figure 2 with no high energy break point. The integral spectrum from the actual fit is also displayed as the black line. Only HiRes-I values (in red) are used to make an estimate of $E_{1/2}$, interpolating between the central value and one standard deviation limits.

In summary, we have measured the flux of ultrahigh energy cosmic rays with the fluorescence technique, in the energy range $10^{17.2}$ to above $10^{20.5}$ eV. We observe two breaks in the energy spectrum corresponding to the GZK cutoff and the ankle. The statistical significance of the break identified with the GZK cutoff is ~ 5 standard deviations. We measure the energy of the GZK cutoff to be $(5.6 \pm 0.5 \pm 0.9) \times 10^{19}$ eV, where the first uncertainty is statistical and the second is systematic.

This work has been supported by US NSF grants PHY-9100221, PHY-9321949, PHY-9322298, PHY-9904048, PHY-9974537, PHY-0073057, PHY-0098826, PHY-0140688, PHY-0245428, PHY-0305516, PHY-0307098, PHY-0649681, and PHY-0703893, and by the DOE grant FG03-92ER40732. We gratefully acknowledge the contributions from the technical staffs of our home institutions. The cooperation of Colonels

E. Fischer, G. Harter and G. Olsen, the US Army, and the Dugway Proving Ground staff is greatly appreciated.

References

- [1] K. Greisen, Phys. Rev. Lett. **16**, 748 (1966).
- [2] G. T. Zatsepin and V. A. Kuz'min, J. Exp. Theor. Phys. Lett. **4**, 78 (1966), [ZhETF Pis'ma **4** (1966) 114–117].
- [3] R. U. Abbasi et al., Phys. Rev. Lett. (2007), submitted, [astro-ph/0703099].
- [4] R. U. Abbasi et al., Astropart. Phys. **23**, 157 (2005), [astro-ph/0208301].
- [5] R. U. Abbasi et al., Physics Letters B **619**, 271 (2005), [astro-ph/0501317].
- [6] C. Song et al., Astropart. Phys. **14**, 7 (2000), [astro-ph/9910195].
- [7] T. K. Gaisser and A. M. Hillas, in *Proceedings of the 15th ICRC* (1977), vol. 8, pp. 353–357.
- [8] T. Abu-Zayyad et al., Astropart. Phys. **16**, 1 (2001), [astro-ph/0008206].
- [9] T. Abu-Zayyad et al., Phys. Rev. Lett. **84**, 4276 (2000).
- [10] R. U. Abbasi et al., Astrophys. J. **622**, 910 (2005), [astro-ph/0407622].
- [11] R. U. Abbasi et al., Astropart. Phys. **27**, 370 (2007), [astro-ph/0607094].
- [12] F. Kakimoto et al., Nucl. Inst. Meth. A **372**, 527 (1996).
- [13] M. Nagano et al., Astropart. Phys. **20**, 293 (2003), [astro-ph/0303193].
- [14] J. W. Belz et al., Astropart. Phys. **25**, 129 (2006), [astro-ph/0506741].
- [15] R. U. Abbasi et al., Astropart. Phys. **25**, 74 (2006), [astro-ph/0512423].
- [16] R. U. Abbasi et al., Astropart. Phys. **25**, 93 (2006), [astro-ph/0601091].
- [17] D. R. Bergman, Nucl. Phys. B Proc. Supl. **165**, 19 (2007), [astro-ph/0609453].
- [18] M. Takeda et al., Astropart. Phys. **19**, 447 (2003), [astro-ph/0209422].
- [19] W.-M. Yao et al., J. Phys. **G 33**, 302 (2006).
- [20] V. S. Berezhinsky and S. I. Grigor'eva, Ast. and Astrophys. **199**, 1 (1988).